Journal of the Korean Society of Surveying, Geodesy, Photogrammetry and Cartography
Vol. 37, No. 5, 351-357, 2019
https://doi.org/10.7848/ksgpc.2019.37.5.351

ISSN 1598-4850(Print)
ISSN 2288-260X(Online)
Original article

Forest Fire Damage Assessment Using UAV Images: A Case Study on Goseong-Sokcho Forest Fire in 2019

Yeom, Junho [1] · Han, Youkyung [2] · Kim, Taeheon [3] · Kim, Yongmin [4]

Abstract

UAV (Unmanned Aerial Vehicle) images can be exploited for rapid forest fire damage assessment by virtue of UAV systems' advantages. In 2019, catastrophic forest fire occurred in Goseong and Sokcho, Korea and burned 1,757 hectares of forests. We visited the town in Goseong where suffered the most severe damage and conducted UAV flights for forest fire damage assessment. In this study, economic and rapid damage assessment method for forest fire has been proposed using UAV systems equipped with only a RGB sensor. First, forest masking was performed using automatic elevation thresholding to extract forest area. Then ExG (Excess Green) vegetation index which can be calculated without near-infrared band was adopted to extract damaged forests. In addition, entropy filtering was applied to ExG for better differentiation between damaged and non-damaged forest. We could confirm that the proposed forest masking can screen out non-forest land covers such as bare soil, agriculture lands, and artificial objects. In addition, entropy filtering enhanced the ExG homogeneity difference between damaged and non-damaged forests. The automatically detected damaged forests of the proposed method showed high accuracy of 87%.

Keywords : Forest Fire, Damage Assessment, ExG, Entropy Filtering, UAV

1. Introduction

Benefits of UAV (Unmanned Aerial Vehicle) systems enable rapid and high-resolution forest fire damage assessment. UAV images can be acquired immediately after forest fire unlike traditional remote sensing data such as satellite images and airborne photos. Revisit time of satellite monitoring systems degrades prompt post-disaster data acquisition. In case of airborne systems, they requires more flight resources and strict compliance with complex regulations than UAV surveying. On the contrary to this, UAV systems require less human resources and cost and can be exploited in time. Since timely data acquisition is the most important factor for disaster damage assessment, UAV systems are getting higher attention from the society and academic fields. The potential of UAV applications in various disaster types has been investigated in recent years. Bhardwaj *et al.* (2016) examined applications of UAV and their prospects in glaciology. They remarked that UAVs' stereo-viewing capabilities can help detect changes in glacier surface elevations. Yang *et al.* (2018) proposed a classification method to identify aquaculture facilities damaged by a typhoon using UAVs. Zhang *et al.* (2018) proposed a framework that utilizes a UAV-based hyperspectral image to identify insect-induced forest damages at tree level. Xu *et al.* (2018) presented a classification method for earthquake damage mapping from UAV photogrammetric point clouds. It can be confirmed from the previous studies that UAV remote sensing enables fine-scale analysis for each specific disaster monitoring theme.

Received 2019. 09. 25, Revised 2019. 10. 11, Accepted 2019. 10. 22
1) Member, Dept. of Civil Engineering, Gyeongsang National University (E-mail: junho.yeom@gnu.ac.kr)
2) Member, School of Convergence & Fusion System Engineering, Kyungpook National University (E-mail: han602@knu.ac.kr)
3) Member, Dept. of Geospatial Information, Kyungpook National University (E-mail: rlaxogjs73@knu.ac.kr)
4) Corresponding Author, Member, LX Spatial Information Research Institute (E-mail: lovefortajo@gmail.com)

On April 4th, 2019, catastrophic forest fire occurred in Goseong, Korea and spread to Sokcho which is about 25 km away due to strong wind. Damaged forest area totaled 1,757 hectares and hundreds of properties including houses, agriculture facilities, and vehicles disappeared. There were many attempts to monitor forest fire damage using remote sensing data. Chu and Guo (2014) reviewed related articles and summarized them based on sensor type and spatial resolution (Kasischke *et al.*, 2011; Loboda *et al.*, 2012; Potapov *et al.*, 2008; Ruiz *et al.*, 2012). Most of the previous research used satellite sensors and their spatial resolutions range from 2.5 m to 8 km, which is quite coarser than UAV images. Airborne LiDAR (Light Detection and Ranging) and SAR (Synthetic Aperture Radar) data were also used for obtaining forest structural information and might address some issues of passive optical systems, however, it is not sufficient for forest monitoring in terms of vegetation greenness. UAV-based fine-scale forest fire monitoring should be investigated so that forest fire damage assessment can be diversified according to the level of detail and research purpose. Yuan *et al.* (2015) investigated UAV-based forest fire monitoring studies over the last decade, however, the problem is that most of the studies focused on the confirmation of forest fire occurrence and localization (Bradley and Taylor, 2011; Martínez-de Dios *et al.*, 2011; Merino *et al.*, 2012). They focused on disaster response, not on surveying-level damage assessment. Therefore, in this study, UAV-based forest fire damage assessment was investigated at fine-scale considering vegetation index and its homogeneity.

We visited the town in Goseong where suffered the most severe damage and conducted UAV flights for data collection. The purpose of this study is developing an economic and rapid damage assessment method for forest fire which can be applied to UAV systems equipped with only a RGB sensor. In this study, ExG (Excess Green) vegetation index which showed good performance in vegetation monitoring in previous research (Torres-Sánchez *et al.*, 2014; Bendig *et al.*, 2015) was adopted to extract damaged forests. Yeom *et al.* (2019) also confirmed that the use of ExG is promising compared to other RGB (Red Green Blue) vegetation indices.

2. Methods

The overall study flow is shown in Fig. 1. UAV orthophoto and DEM (Digital Elevation Model) were generated from UAV raw images. For the processing, ground coordinates of GCPs (Ground Control Points) were added as constraints for accurate geo-rectification. Then, forest areas were extracted based on the DEM to mask out non-forest land covers such as bare soil, agricultural lands, paved roads, and artificial objects. The elevation criterion for the forest area filtering was automatically calculated by Otsu algorithm. Then, ExG vegetation index on the filtered forest area was calculated. For extraction of damaged forest, entropy filtering was additionally applied to the ExG result and thresholding value between damaged and non-damaged forests was derived using Otsu algorithm.

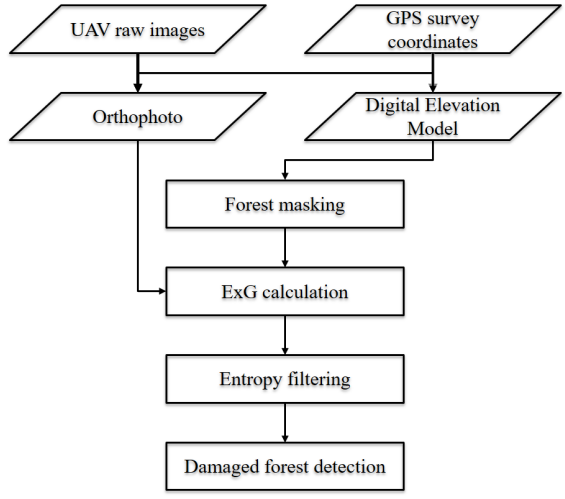

Fig. 1. Flowchart of the study

2.1. UAV data processing and forest masking

Two months after the Goseong-Sokcho forest fire, UAV flight was conducted using DJI Inspire 2 and Zenmuse X4S RGB sensor. UAV raw images were collected at 60 m altitude with a 70% overlap. Before the flight, eight ground targets were distributed and their coordinates were measured by ground GPS (Global Positioning System) surveying. From

the acquired UAV raw images, orthophoto and DEM were generated using Agisoft Photoscan software.

From the generated DEM, threshold value that separates forest and others was automatically calculated using Eq. (1). It was assumed that high elevation regions in a small study site correspond with forests since the elevation change due to mountain area is considerably higher than plain elevation change. As in Eq. (1), total variance (σ^2) can be divided into in-class variance (σ_i^2) and inter-class variance (σ_b^2). Otsu algorithm determines threshold value (t) that maximizes inter-class variance thereby minimizing in-class variance. The in-class variance is defined by the weighted sum of each class variance as in Eq. (2). In this study, class 1 and 2 represent forest and others, respectively. The threshold value minimizes in-class variance was determined automatically. In addition, a histogram of DEM was checked since Otsu algorithm assumes bi-modal distribution of input data.

$$\sigma^2 = \sigma_i^2 + \sigma_b^2 \tag{1}$$

$$\sigma_i^2(t) = w_1(t)\sigma_1^2(t) + w_2(t)\sigma_2^2(t) \tag{2}$$

where w_1 and w_2 are weight coefficients for class 1 and 2, σ_1^2 and σ_2^2 are variances of class 1 and 2.

2.2. ExG calculation and entropy filtering

Near-infrared vegetation indices are mainly used for forest research. However, RGB vegetation indices showed promising results in the previous study compared with near-infrared vegetation indices (Yeom *et al.*, 2019) and forest fire damage assessment using RGB images is required for versatile application and rapid countermeasures. Therefore, ExG RGB vegetation index was adopted in this study and the formula is shown in Eqs. (3) and (4).

$$\mathrm{ExG} = 2G_n - R_n - B_n \tag{3}$$

$$R_n = \frac{R}{R+G+B}, \quad G_n = \frac{G}{R+G+B}, \quad B_n = \frac{B}{R+G+B} \tag{4}$$

The generated ExG image was clipped based on the result of forest masking. In addition, entropy filtering was applied to the ExG image in order to consider forest homogeneity. Entropy (H) is the measure of uncertainty or mixedness defined by Eq. (5). In this study, it was assumed that non-damaged forest has higher entropy than damaged forest because leaves, shadows, and branches are mixed up before forest fire, which results in high entropy. Conversely, exposed bare ground or ground covered by ashes has relatively homogeneous textures, which results in low entropy.

$$H = -\sum_{i=1}^{n} P(e_i)\log P(e_i) \tag{5}$$

where e_i and P_i are an event element and its probability, respectively. The entropy filtering was performed using a 11 by 11 moving window, therefore, noisy clutters resulted from cm-level UAV images were suppressed while calculating averaged local entropy.

2.3. Damaged forest detection and accuracy assessment

Otsu algorithm was applied to the ExG entropy filtering result for the detection of damaged forests. Low ExG entropy regions were regarded as damaged forest and the threshold value that separate damaged and non-damaged forests was automatically determined by Eqs. (1) and (2). In addition, the result was compared with the damaged forest detected from the ExG without entropy filtering for verification of entropy filtering. Histograms of ExG entropy and original ExG were compared with each other to check probability density.

Since UAVs allow super high-resolution imaging and the images contain every single detail, patch-based accuracy assessment was performed. First, accurate forest areas were manually digitized and 100 patches in the digitized data were randomly extracted. The size of each patch is 1 m by 1 m. After random patch extraction, each patch was labeled as damaged forest or non-damaged forest by image interpretation. These reference data were compared with forest fire damage assessment results from the proposed method which uses ExG and entropy filtering together. In our forest fire damage assessment, when the ratio of damaged forest pixels on the patch is higher than 50%, the patch is then determined as a damaged forest.

3. Results and Discussion

3.1 Experimental Data

We visit Toseong town in Goseong, Korea on May 27. DJI Inspire 2 platform and Zenmuse X4S RGB sensor were used for UAV data collection. A total of 404 raw images were collected and the coverage area was 0.113 km^2. A part of the covered area was selected as a study site which is 42,000 m^2 (Fig. 2(a)). The generated orthophoto and DEM have spatial resolutions of 1.49 cm and 5.97 cm, respectively (Fig. 2). It can be observed from Fig. 2(a) that there was severe forest fire damage on the forest.

(a) (b)

Fig. 2. UAV data of the study site (a) Orthophoto, (b) DEM

3.2 Results

Histogram of DEM elevation in the study site is shown in Fig. 3(a). It describes the probability density of DEM elevation and follows bi-modal distribution which is the assumption of Otsu algorithm. The automatically derived threshold value was 37.7463 m, which corresponds to the valley between two peaks: (1) more frequent and lower elevation on the plain, (2) less frequent and higher elevation on the mountain area. The extracted forest area is shown in Fig. 3(b). Although the entire forest area was well extracted, some high buildings and trees were extracted as forest area since parts of trees and buildings have a higher elevation than the threshold value of 37.7463 m as shown in Fig. 4(a) and 4(b). In addition, the DEM derived from UAV images has an inevitable problem with conjugate point matching on some trees since trees move by wind, which resulted in the omission of DEM data. For these regions, it is not able to extract forest area since DEM data are not available (Fig. 4(c)).

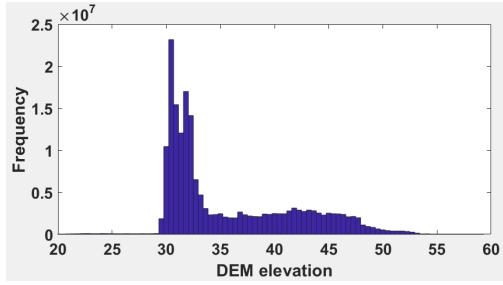

(a)

(b)

Fig. 3. Forest masking (a) Histogram of DEM elevation, (b) Extracted forest area

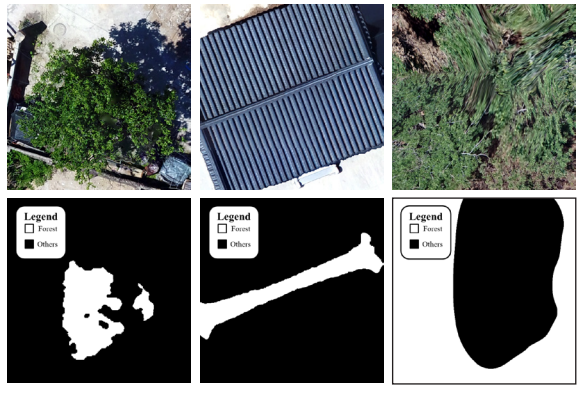

(a) (b) (c)

Fig. 4. Errors in forest masking (a), (b) commission error, (c) omission error

ExG vegetation index calculation and its entropy filtering results are shown in Fig. 5. Other land covers except for forests were masked out using the previous forest masking results. ExG values are generally between –1 and 1 like other vegetation indices as shown in Fig. 5(b). Although damaged forest areas are visually obvious in Fig. 2(a), ExG difference between damaged and non-damaged forests is not clear

and most of the values are concentrated around the value of 0 (Fig. 5(a) and (b)). On the contrary to this, the entropy filtering result showed better contrast than the original ExG (Fig. 5(c)). Moreover, the value of ExG entropy is distributed along the entire range between 0 and 7 forming bi-modal distribution (Fig. 5(d)): (1) dominant lower ExG entropy from the damaged forests, (2) a minority of non-damaged forests that have higher ExG entropy.

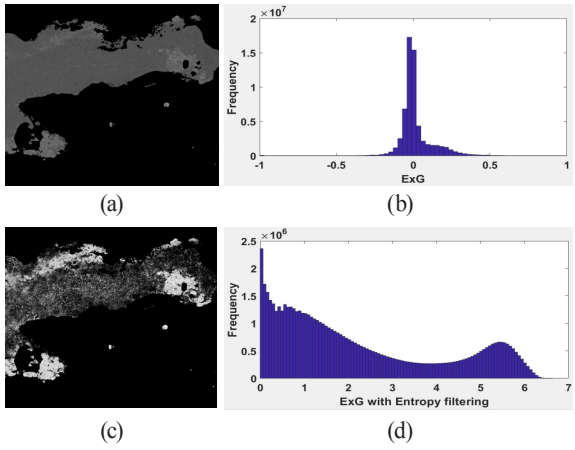

(a) (b)

(c) (d)

Fig. 5. ExG calculation and entropy filtering (a) ExG in the forest areas, (b) Distribution of ExG, (c) Entropy filtering results in the forest areas, (d) Distribution of ExG entropy

The threshold values for ExG and ExG entropy were automatically determined and the values were 0.1059 and 2.9172, respectively. Based on the threshold values, low ExG and low ExG entropy areas were detected as damaged forests, respectively (Fig. 6). The main difference between the results was that ExG-based damage detection is more sensitive to single-pixel details than the result of ExG entropy filtering. This can be confirmed from the enlarged visual comparison in Fig. 7(d)–(f). The detected damaged forest from ExG was sensitive to pixel-level noises on the ground, branches, and withered leaves. Conversely, the result from the proposed ExG entropy filtering was able to detect damaged forests considering homogeneity of neighboring regions (Fig. 7).

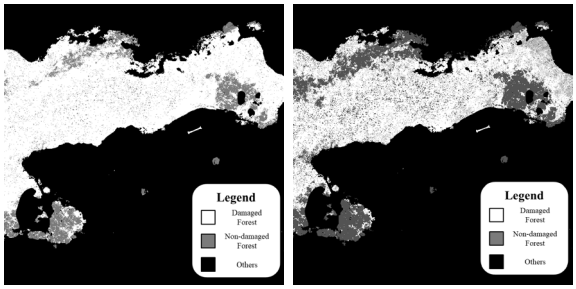

(a) (b)

Fig. 6. Damaged forest detection (a) ExG, (b) ExG entropy

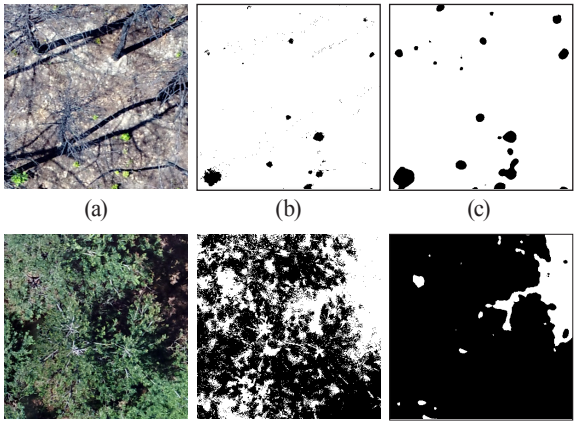

(a) (b) (c)

(d) (e) (f)

Fig. 7. Enlarged images for visual comparison (white: damaged forest, black: non-damaged forest) (a), (d) orthophoto, (b), (e) damaged forest from ExG, (c), (f) damaged forest from ExG entropy filtering

Hundred patches in the reference forest area were randomly extracted and then interpreted to label them as damaged forest or non-damaged forest. The labeled patches were compared with automatic forest damage decisions derived from the damaged forest ratio. The accuracy assessment result is shown in Table 1. The proposed method, ExG entropy filtering, showed 87% overall accuracy of forest fire damage detection. The proposed method rarely extracted wrong damaged forest. However, the proposed method sometimes overestimates non-damaged forests. It is because entropy filtering is sensitive to the presence of vegetation and shadow pixels. A few green leaves and shadows can increase the entropy values of a moving window, which resulted in the overestimation of non-damaged forests as in the right

figure of Fig. 8(c). In addition, failure of the forest area filtering affected the omission of damaged forest detection as in the left figure of Fig. 8(c). Fig. 8 shows the examples of correct damaged forest detection, correct non-damaged forest detection, and overestimation of non-damaged forests.

Table 1. Accuracy of the proposed forest fire damage assessment

Type		Reference data	
		Damaged forest	Non-damaged forest
The proposed method (ExG with entropy filtering)	Damaged forest	53	-
	Non-damaged forest	13	34

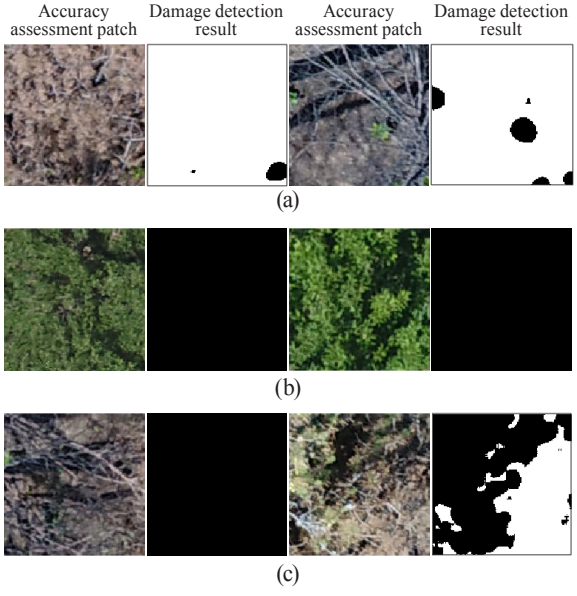

Fig. 8. Examples of accuracy assessment patches and forest fire damage detection from the proposed method (white: damaged forest, black: non-damaged forest) (a) correct damaged forest detection, (b) correct non-damaged forest detection, (c) overestimation of non-damaged forests

4. Conclusion

In this study, a UAV-based fine-scale forest fire damage assessment was investigated. First, forest areas were automatically extracted based on the elevation threshold value. Then ExG RGB vegetation index was calculated so that the proposed forest fire damage assessment can be applied to standard RGB sensor without near-infrared information. In addition, entropy filtering was applied to the ExG result for better identification of damaged forests.

The advantages of the proposed method are as follows. First, the proposed method can be an effective solution for rapid forest fire damage assessment using consumer-grade UAV RGB sensors. Second, the proposed method confirmed that the use of only a vegetation index is not enough for accurate forest fire damage assessment due to ambiguity in determination of a threshold value between damaged and non-damaged forests. The application of entropy filtering improved forest damage detection accuracy by considering vegetation index textures. The proposed forest masking method may not work well on different study sites where have steep plain. Therefore, as future works, elevation and slope combined factors will be investigated for versatile application. Additionally, 3D analysis approach will be developed for volumetric forest fire damage assessment.

Acknowledgment

This work was supported by the National Research Foundation of Korea (NRF) grant funded by the Korea government (MSIP) (2017R1C1B2005744) and This research was supported by Basic Science Research Program through the National Research Foundation of Korea (NRF) funded by the Ministry of Education (2018R1A6A3A01010972).

Reference

Bendig, J., Yu, K., Aasen, H., Bolten, A., Bennertz, S., Broscheit, J., Gnyp, M.L., and Bareth, G. (2015), Combining UAV-based plant height from crop surface models, visible, and near infrared vegetation indices for biomass monitoring in barley, *International Journal of Applied Earth Observation and Geoinformation*, Vol. 39, pp. 79–87.

Bhardwaj, A., Sam, L., Martín-Torres, F.J., and Kumar, R. (2016), UAVs as remote sensing platform in glaciology: Present applications and future prospects, *Remote sensing*

of environment, Vol. 175, pp. 196–204.

Bradley, J.M. and Taylor, C.N. (2011), Georeferenced mosaics for tracking fires using unmanned miniature air vehicles, *Journal of Aerospace Computing, Information, and Communication*, Vol. 8, No. 10, pp. 295–309.

Chu, T. and Guo, X. (2014), Remote sensing techniques in monitoring post-fire effects and patterns of forest recovery in boreal forest regions: A review, *Remote Sensing*, Vol. 6, No. 1, pp. 470–520.

Kasischke, E.S., Loboda, T., Giglio, L., French, N.H., Hoy, E.E., de Jong, B., and Riano, D. (2011), Quantifying burned area for North American forests: Implications for direct reduction of carbon stocks. *Journal of Geophysical Research: Biogeosciences*, Vol. 116, G4

Loboda, T.V., Zhang, Z., O'Neal, K.J., Sun, G., Csiszar, I.A., Shugart, H.H., and Sherman, N.J. (2012), Reconstructing disturbance history using satellite-based assessment of the distribution of land cover in the Russian Far East, *Remote sensing of environment*, Vol. 118, pp. 241-248.

Martínez-de Dios, J., Merino, L., Caballero, F., and Ollero, A. (2011), Automatic forest-fire measuring using ground stations and unmanned aerial systems, *Sensors*, Vol. 11, No. 6, pp. 6328–6353.

Merino, L., Caballero, F., Martínez-De-Dios, J.R., Maza, I., and Ollero, A. (2012), An unmanned aircraft system for automatic forest fire monitoring and measurement, *Journal of Intelligent & Robotic Systems*, Vol. 65, No. 1–4, pp. 533–548.

Potapov, P., Hansen, M.C., Stehman, S.V., Loveland, T.R., and Pittman, K. (2008), Combining MODIS and Landsat imagery to estimate and map boreal forest cover loss, *Remote Sensing of Environment*, Vol. 112, No. 9, pp. 3708–3719.

Ruiz, J.A.M., Riaño, D., Arbelo, M., French, N.H., Ustin, S.L., and Whiting, M.L. (2012), Burned area mapping time series in Canada (1984–1999) from NOAA-AVHRR LTDR: A comparison with other remote sensing products and fire perimeters, *Remote Sensing of Environment*, Vol. 117, pp. 407–414.

Torres-Sánchez, J., Peña, J.M., De Castro, A.I., and López-Granados, F. (2014), Multi-temporal mapping of the vegetation fraction in early-season wheat fields using images from UAV, *Computers and Electronics in Agriculture*, Vol. 103, pp. 104–113.

Xu, Z., Wu, L., and Zhang, Z. (2018), Use of active learning for earthquake damage mapping from UAV photogrammetric point clouds, *International journal of remote sensing*, Vol. 39, No. 15-16, pp. 5568–5595.

Yang, M.D., Huang, K.S., Wan, J., Tsai, H.P., and Lin, L.M. (2018), Timely and quantitative damage assessment of oyster racks using UAV images. *IEEE Journal of Selected Topics in Applied Earth Observations and Remote Sensing*, Vol. 11, No. 8, pp. 2862–2868.

Yeom, J., Jung, J., Chang, A., Ashapure, A., Maeda, M., Maeda, A., and Landivar, J. (2019), Comparison of vegetation indices derived from UAV data for differentiation of tillage effects in agriculture, *Remote Sensing*, Vol. 11, No. 13, pp. 1548.

Yuan, C., Zhang, Y., and Liu, Z. (2015), A survey on technologies for automatic forest fire monitoring, detection, and fighting using unmanned aerial vehicles and remote sensing techniques, *Canadian Journal of Forest Research*, Vol. 45, No. 7, pp. 783–792.

Zhang, N., Zhang, X., Yang, G., Zhu, C., Huo, L., and Feng, H. (2018), Assessment of defoliation during the Dendrolimus tabulaeformis Tsai et Liu disaster outbreak using UAV-based hyperspectral images, *Remote Sensing of Environment*, Vol. 217, pp. 323–339.